

Study of the phase transition in the 3d Ising spin glass from out of equilibrium numerical simulations

S. P.erez G aviro yz, Juan J. R uiz-Lorenzo xz and A .Tarancon yz

yD epartam ento de F ísica Teórica, Facultad de C iencias, Universidad de Zaragoza, 50009 Zaragoza, Spain.

xD epartam ento de F ísica, Facultad de C iencias, Universidad de Extrem adura, 06071 Badajoz, Spain.

zInstituto de B iocom putación y F ísica de Sistem as C om plejps (B IF I), Corona de Aragón 42, 50009 Zaragoza, Spain

E-m ail: spgaviro@unizar.es, ruiz@unex.es, tarancon@unizar.es

A bstract. U sing the decay of the out equilibrium spin-spin correlation function we com pute the equilibrium Edward-Anderson order param eter in the three dim ensional binary Ising spin glass in the spin glass phase. W e have checked that the Edward-Anderson order param eter com puted from out of equilibrium numerical simulations follows with good precision the critical law as determ ined in experim ents and in numerical studies at equilibrium (which allow us to estim ate the critical exponent). Finally we present a large tim e study of the o -equilibrium fluctuation-dissipation relations and we nd strong discrepancies (in the low tem perature region) between the numerical data and the droplet theory predictions and agreem ent w ith the predictions of the replica sym m etry breaking theory.

PACS num bers: 05.70 Ln, 75.10 Nr, 75.40 M g

1. Introduction

The characterization, using numerical simulations, of the phase transition in the three dimensional Ising spin glasses has been a challenging problem. Recently a clear picture of the phase transition and good estimates of the critical exponents have been obtained for both Gaussian and bimodal disorder by working at equilibrium [1, 2, 3].

However a characterization of the phase transition using out of equilibrium techniques is still lacking (see reference [4] for a detailed discussion). In the first part of this paper we will address this problem (simulating the bimodal disorder). In particular we will compute the order parameter using out of equilibrium techniques [5] and we will characterize the transition using this observable. In addition we will confront our data with previous estimates of the critical point and critical exponents for this model (obtained from numerical simulations and from experiments). The behavior of this observable will permit us to discard (again) a Kosterlitz-Thouless like phase transition (as done in equilibrium [1], that we will refer in the following as XY-like scenario) for the transition [4]. Moreover, we have studied the dependence of the order parameter with the size of the system. Hence, we will present on this paper the first direct numerical computation of the Edwards-Anderson order parameter in the three dimensional Ising spin glass (obtained out of equilibrium).

This kind of study was performed in the past in four dimensions [6] (see also [7, 8]) but is still lacking in three dimensions (the interesting physical dimensions).

The second part of the paper is devoted to the study of the fluctuation-dissipation theorem out of equilibrium. This kind of analysis have attracted a large amount of work (analytical, numerical and experimental) in the last years [9, 10, 11, 12, 13, 14].

Using the results of reference [14] and assuming that the three dimensional Ising spin glass presents stochastic stability (until now it has not been rigorously proved but there are numerical evidences [17]) one can relate the fluctuation-dissipation curves with equilibrium properties and so, compute or measure the equilibrium probability distribution of the overlap. This computation or measurement is very important since it should discern between the different theoretical approaches in competition, which try to describe the behavior of finite dimensional spin glasses (e.g. the Replica Symmetry Breaking (RSB) approach [16, 17] or the droplet model [18]).

The goal of this (last) part of the paper is twofold. First, to check if the order parameter computed in the first part of this paper matches well in the fluctuation-dissipation (FD) curves. This is important since this value marks the point in which the FD curve departs from its pseudo-equilibrium regime, and the behavior of the curve from this departing point is a clear fingerprint whether or not the system behaves following the RSB theory or the droplet model.

And the second goal is to study the finite time behavior (for really large times) of the curves in order to see how the asymptotic form of the FD curves is built up. This is important, since until now, the numerical simulations [12] and experiments [15] show up a behavior compatible with the Replica Symmetry Breaking description

and incompatible with droplet theory. One can argue that the curves reported in the literature [12, 15] are not asymptotic and that the asymptotic curve is compatible with droplet theory and not compatible with RSB.

Finally, we will report the conclusions.

2. The model and Numerical simulations

We have simulated a three dimensional system in a cubic lattice with helicoidal boundary conditions of size L and volume $V = L^3$. The Hamiltonian is

$$H = \sum_{\langle i;j \rangle} J_{ij} \sigma_i \sigma_j; \quad (1)$$

where $\langle i;j \rangle$ denotes the sum over the first nearest neighbors, $\sigma_i = \pm 1$ are Ising variables and $J_{ij} = \pm 1$ are quenched random variables with a binodal probability distribution with zero mean and unit variance. We have used the standard heat-bath algorithm (local dynamics) to simulate the three-dimensional lattice.

We will introduce the observables measured in our work. Firstly, the order parameter (the Edwards Anderson one) is defined as:

$$q_{EA} = \overline{h_i^2}; \quad (2)$$

where, as usual, we use $h(\cdot)$ and $\overline{(\cdot)}$ to denote thermal and quenched disorder average respectively.

In addition, the spin-spin correlation function has been computed using

$$C(t; t_w) = \frac{1}{V} \sum_{i=1}^X \sigma_i(t) \sigma_i(t_w); \quad (3)$$

We can obtain formally the order parameter from this correlation as the double limit:

$$q_{EA} = \lim_{t \rightarrow \infty} \lim_{t_w \rightarrow \infty} C(t; t_w); \quad (4)$$

Notice that the order of the limit is crucial in obtaining the order parameter. We will use this equation to extract q_{EA} from the out-of-equilibrium data.

We will study in the last part of the paper the finite time behavior of the violation of the fluctuation-dissipation relation in the three dimensional spin glass. We will review shortly the main equation of the out-of-equilibrium fluctuation-dissipation equations (see [19] for more details):

$$R(t_1; t_2) = \frac{1}{T} \sum (C(t_1; t_2)) \frac{\partial C(t_1; t_2)}{\partial t_2}; \quad (5)$$

where, $t_1 > t_2$, $R(t_1; t_2)$ is the response of the system to the magnetic field perturbation (i.e. the magnetic susceptibility of the system: $R(t_1; t_2) = m(t_1; t_2) = h$) and $X(C)$ is the, in principle unknown, function which controls the violation of the fluctuation-dissipation theorem. Integrating this equation in t_2 and taking the perturbing field as $h(t) = h(t - t_w)$ we finally obtain (working in the linear-response region):

$$m(t) = \int_{C(t; t_w)}^Z h(u) X(u) du; \quad (6)$$

In the regime $t_1 < t_2 < 1$ we reach the equilibrium, and it is possible to show that $C(t_1; t_2) \sim q$. In addition $X(q) \sim \int_{q_{min}}^q dq P(q)$, where $X(q)$ is the integral of the probability distribution of the overlap at equilibrium [16]. Hence, in this regime [9, 10, 11, 12, 13, 14],

$$m(t) = \frac{1}{Z} \int_{C(t; t_w)} du X(u) \quad (7)$$

Furthermore, we can define

$$S(C) = \int_{C(t; t_w)} dq X(q) \quad (8)$$

so,

$$\frac{m(t)T}{h} = S(C(t; t_w)) \quad (9)$$

Both, in droplet theory and RSB (see reference [21], in particular its figure 10), $S(C)$ is the straight line $1 - C$ for $C \geq q_{EA}$. However, for $C < q_{EA}$ the behavior is very different: in the droplet theory $S(C)$ is constant in this region and in RSB $S(C)$ is a growing function with curvature. We recall that knowing the initial point, $S(C = 0)$, we can compute q_{EA} in the droplet theory as

$$q_{EA}^{droplet} = 1 - S(C = 0) \quad (10)$$

This technique allows us to compute, taking the appropriate limit, the equilibrium function $X(q)$.

Finally, we report that all the numerical simulations have been obtained with the SUE machine [22]. This is a dedicated machine, designed for the simulation of the three dimensional Edwards-Anderson model with first neighbour couplings [16], the system that is being studied in the present work. It consists of 12 identical boards. Each single board is able to simulate 8 different systems, updating all of them at each clock cycle. SUE reaches an update speed of 217 ps/spin with a clock frequency of 48 MHz. The on-board reprogrammability permits to change in an easy way the lattice size, or even the update algorithm or the Hamiltonian. The SUE machine is connected to a Host Computer running under Linux. SUE is in charge of the update of the configurations, and the host computer is in charge of measurements and analysis. The main electronic devices of each SUE board are the Altera family, that performs the update. Other devices store the spins and couplings variables. One of the Alteras is devoted to generate random numbers in a fast way (for more details, see Ref. [22]). Up to our knowledge, SUE has been the fastest dedicated machine in the simulation of the three dimensional Edwards-Anderson model.

3. Computation of the Edwards-Anderson Order Parameter

In order to compute the Edwards-Anderson order parameter (q_{EA}), we have carried out several runs for two lattice sizes and different temperatures: $\beta = 1/T = 2.00, 1.67, 1.25, 1.05, 1.00, 0.95$ and 0.91 for $L = 30$; and $\beta = 2.00; 1.67; 1.25$ and 1.00 for $L = 60$. For

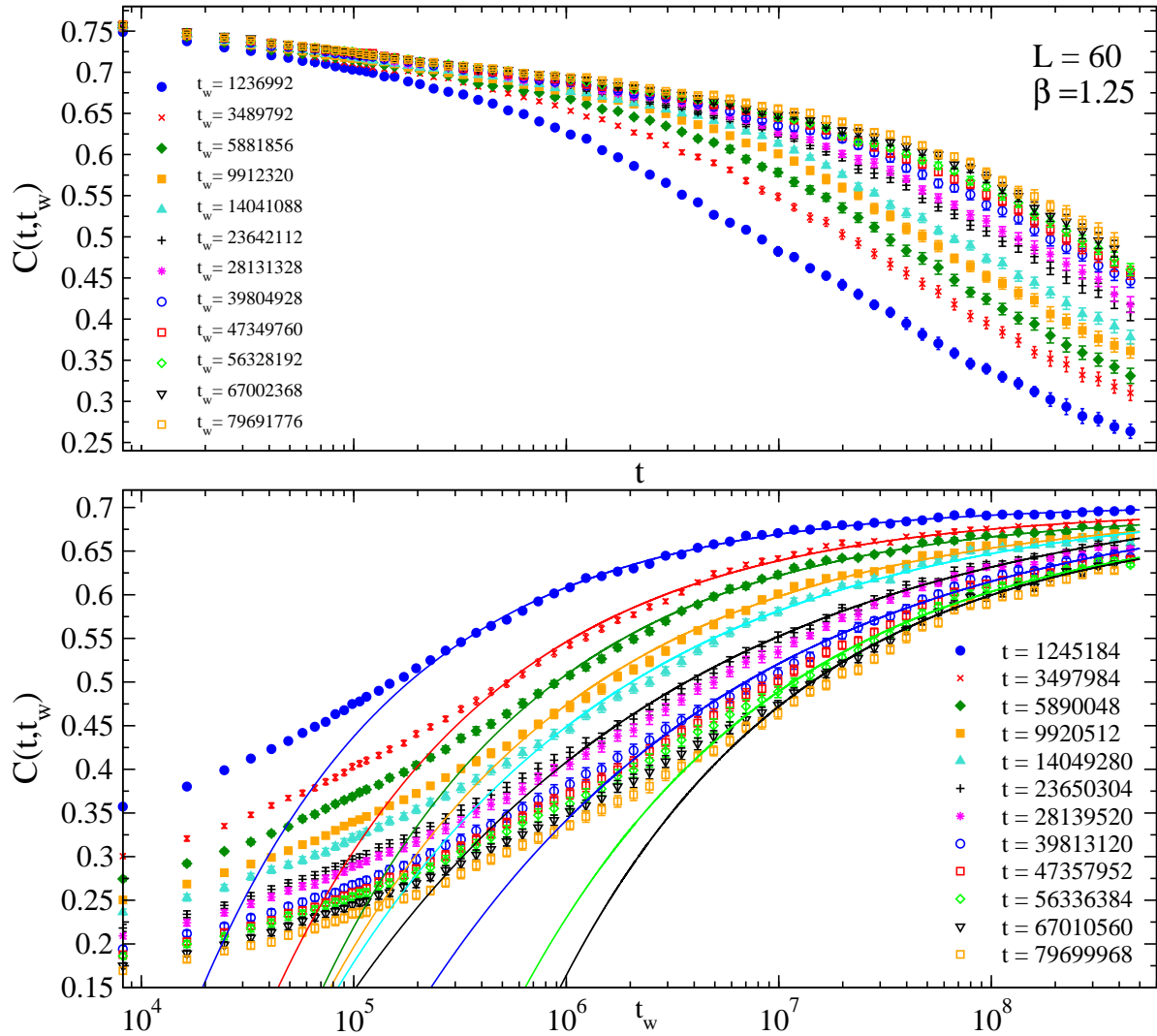


Figure 1. Out of equilibrium spin-spin correlation function $C(t; t_w)$ computed for $L = 60$ and $\beta = 1.25$. Top: $C(t; t_w)$ versus time, t . Bottom: $C(t; t_w)$ versus waiting time, t_w , obtained by studying figure in top for several fixed times t in order to find the limit $t_w \rightarrow \infty$ behavior of $C(t; t_w)$. The continuous lines in the plot are the fits to equation (11). Notice that for the curves with larger waiting time we have chosen to show not all the fits to (11) in order to present a clean figure (the quality of the fits is the same for all the waiting times).

all of them we have averaged over 58 samples. In figure (1) we report the curves $C(t; t_w)$ as a function of time t .

We have checked that the behavior of $C(t; t_w)$ for $t_w \rightarrow \infty$ follows with high precision the behavior (as in higher dimensions, see [6, 7]; this is just an Ansatz):

$$C(t; t_w) = a(t) + b(t)t_w^{-c(t)}; \quad (11)$$

where $a(t)$ is related with the value of q_{EA} . In order to find it out we have first obtained, from figure (1) top, the curves $C(t; t_w)$ vs. t_w for several fixed values of t (typically, from 8192 to $3.7 \cdot 10^6$ Monte Carlo steps) (see figure (1) bottom). We have fitted

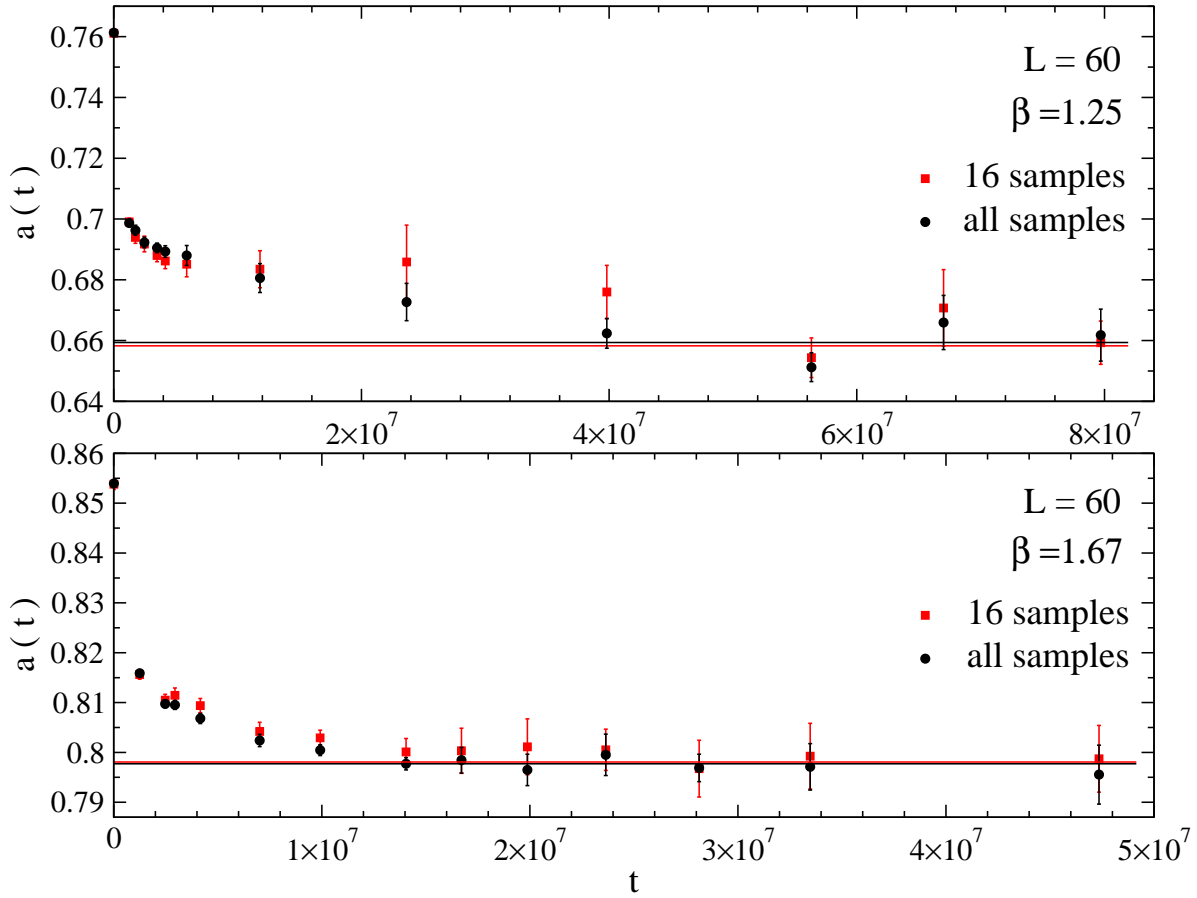


Figure 2. Function $a(t)$ defined in equation (11) computed for $L = 60$ lattice size and $\beta = 1.25$ (top) and $\beta = 1.67$ (bottom). Notice that the last points of the curve can be fitted to a constant in the two plots. In addition we have drawn the function $a(t)$ with only 16 samples in order to show the dependence of the extrapolated value (i.e. the plateau) on the number of samples.

these curves to the functional form defined in (11) obtaining in this way the behavior of $a(t)$ as function of t (we show these fits in figure (1)). From $a(t)$ and for $t \rightarrow 1$, we can obtain the value of q_{EA} (since asymptotically $a(t)$ must become q_{EA}). To achieve this aim, we have fitted the last points of $a(t)$ versus t to a constant function (since $a(t)$ shows a clear plateau, see Fig.(2)). In this way, we have implemented the double limit in equation (4). The results obtained from these fits are shown in Fig.(3).

We have checked that for $\beta > 1.00$ the values for q_{EA} are the same for both $L = 30$ and $L = 60$. In $\beta = 1.00$ the difference is about 1.5 standard deviations. In addition we have run a $L = 20$ lattice at $\beta = 0.91$ and $\beta = 1.00$: these data show finite size effects as expected since they lie near the critical point (see figure(3)).

4. Characterizing the Phase Transition

As we mentioned before, we have checked that the q_{EA} , which we have computed out of equilibrium, follows with good precision the critical law of the order parameter

$$q_{EA}(\beta) = A(\beta - \beta_c)^{\nu} ; \quad (12)$$

where we have denoted ν the usual exponent of the order parameter (in order to avoid confusion with the usual notation $\nu = 1/T$)

By fitting only the points closer to the critical one (satisfying $\beta < 1.25$) we obtain

$$\beta_c = 0.866(2) \quad \nu = 0.52(9) ; \quad (13)$$

with a $\chi^2/\text{d.o.f} = 1.13$. This figures compare really well with the numerical values obtained at equilibrium [1], namely: $\beta_c = 0.88(1)$ and $\nu = 0.71(5)$. In particular the difference between the two estimates of ν is 0.19(11), less than two standard deviations.

In addition, we can compare with experiments. In reference [23] was found $\nu = 0.54(10)$ which is in a very good agreement with our out of equilibrium value.

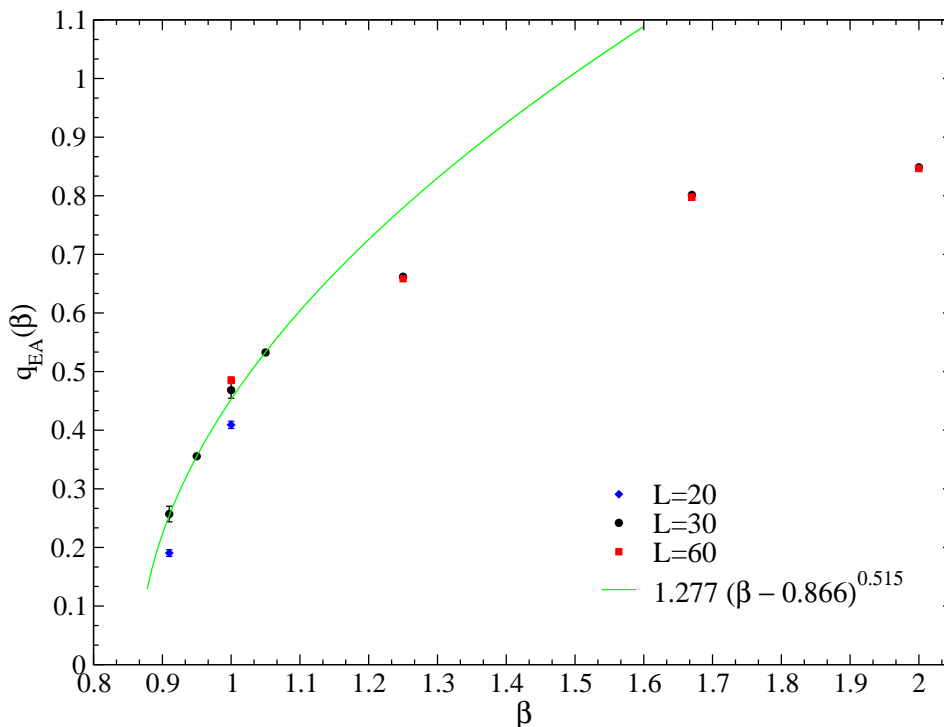


Figure 3. q_{EA}^{dyn} versus β for three lattices sizes $L = 20; 30$ and 60 . The continuous line is the fit reported in the text.

z Notice that in reference [1] corrections to scaling were taken into account. In our estimate there is no scaling corrections, hence our error are smaller than the error quoted in [1]: i.e. our error bars are underestimated.

x See also [24] for a non Universality scenario: they reported $\beta_c = 0.84(1)$.

k Note that both results in [1] and [23] come from different methods.

We have also checked that q_{EA} follows with good precision the critical law

$$(q_{EA}(t))^{1-\nu} = A(t - t_c); \quad (14)$$

Again, we have only used in the fit the points with $t < 1.25$ (critical region). Moreover we can fit q_{EA} to the experimental value, obtaining again a compatible value with the equilibrium one: $t_c = 0.8603(6)$ (236), where the first error is statistical and the second error comes from the error of the experimental q_{EA} . In addition, by fitting q_{EA} to the numerical simulations value we obtain $t_c = 0.820(3)$ (13), less than three standard deviations from the numerical value.

All figures reported in this analysis are compatible with latest estimates of the critical exponents. In reference [2] $\nu = 0.893(3)$ and $\nu_q = 0.723(25)$ were reported. In addition a diluted version of this model was studied in [3] and $\nu_q = 0.723(50)$ was reported.

Finally, we remark that our numerical results from both ν_c and ν_q must suffer from the systematic error coming from the dependence of q_{EA} with L near the critical point (as shown the $L = 20$ runs). At $t = 1.00$ we have three different values of the order parameter that fit to the law

$$q_{EA}(L) = q_{EA}(L_\infty) + \frac{b}{L^c};$$

where b and c are constants. This is the finite volume correction equation which holds in the low temperature phase. We have obtained $c = 3.54$ and $q_{EA}(L_\infty) = 0.49$ (notice that we are fitting three points to a three parameter function) to be compared with $q_{EA}(L = 60) = 0.485(6)$ and $q_{EA}(L = 30) = 0.47(1)$. At $t = 0.91$ (the nearest value we have to the critical point) we have only two points, that anyhow, we can try to fit to equation (4) fitting $c = 3.54$, obtaining $q_{EA}(L_\infty) = 0.278$ (no error bars can be reported since, again, the number of degrees of freedom in this fit is zero) to be compared with the value of our largest lattice $q_{EA}(L = 60) = 0.26(1)$, so this limited analysis suggests that the $L = 30$ lattice is asymptotic in its error bars in the region $t > 0.91$. Hence, we are confident that our final estimates of ν_c and ν_q should have small systematic error coming from finite size effects.

We remark that testing the dependence of q_{EA} with the lattice size, for large lattices (e.g. $L = 60$) near the transition is not accessible even using the SUE machine.

5. Finite Time Effects in the Fluctuation-Dissipation relations

We have performed several runs again with SUE machine, in a lattice of size $L = 60$ for different temperatures: $t = 1.25; 1.10; 1.05; 1.00$ and 0.95 . We have used the following

{ In reference [20] was checked that in the three dimensional Gaussian Ising spin glass the position of the maximum of the equilibrium probability distribution of the overlap follows this law with $c = 1.5(4)$ by fitting $L \leq 16$. Notice that in our case we are using $20 \leq L \leq 60$ data and we simulate the J model and that the exponent could depend on the temperature. Notice that usually in equilibrium small lattices develop larger order parameter, however, in our dynamical approach we have found the opposite behavior.

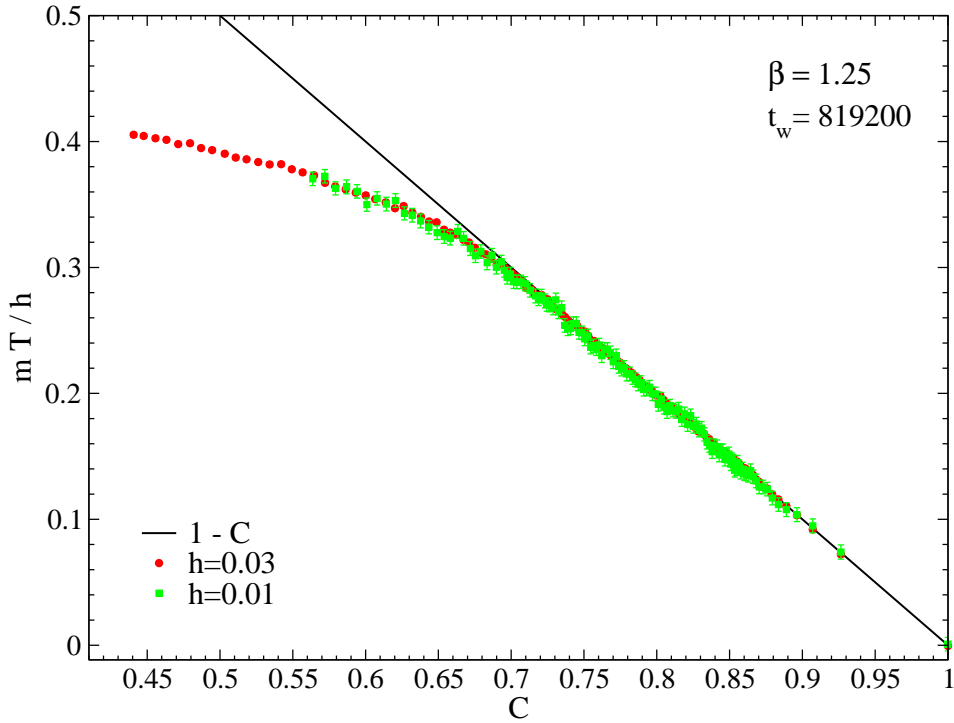


Figure 4. Fluctuation-dissipation curve out of equilibrium for one of the lowest temperature simulated $\beta = 1.25$, $L = 60$ and one waiting time for two different perturbing magnetic fields, $h = 0.01$ and 0.03 , in order to check linear-response.

standard procedure. We let the system evolve during a time t_w , just after this time, a field $h = 0.03$ is plugged, seeing the response of the system and recording the magnetization and the correlation function. Then it is possible to extract the value of q_{EA} , for the particular C being analyzing at that moment, from the point where the curve leaves the linear regime, that is, where mT/h does not follow the pseudo-equilibrium line $(1-C)=T$.

The choice of the field strength applied to the system has not been arbitrary. We need to stay in the linear-response region. We have checked this by simulating different magnetic fields: $h = 0.01; 0.03; 0.05$ and 0.10 . Finally we have selected a safe value for h : $h = 0.03$, which is a compromise between large and small fields (notice that small fields induce strong noise in the measures). In figure (4) we have shown the FDT curve for a waiting time and two perturbing magnetic fields ($h = 0.01$ and 0.003) in order to test that we are in the region in which linear-response holds. It is clear from this figure that the curve, inside the error bars, is independent of the perturbing magnetic field.

In the droplet model, the curve $X(C)$ departs horizontally from the straight line $1-C$, the initial value of the horizontal line being $m_{asyn}T=h$ (i.e. $S(C=0)$), where m_{asyn} is the equilibrium value of the magnetization in a field h at the temperature T . Hence, measuring m_{asyn} we can obtain the droplet theory estimate for the order parameter as:

$$q_{EA}^{droplet} = 1 - \frac{m_{asyn}T}{h} : \quad (15)$$

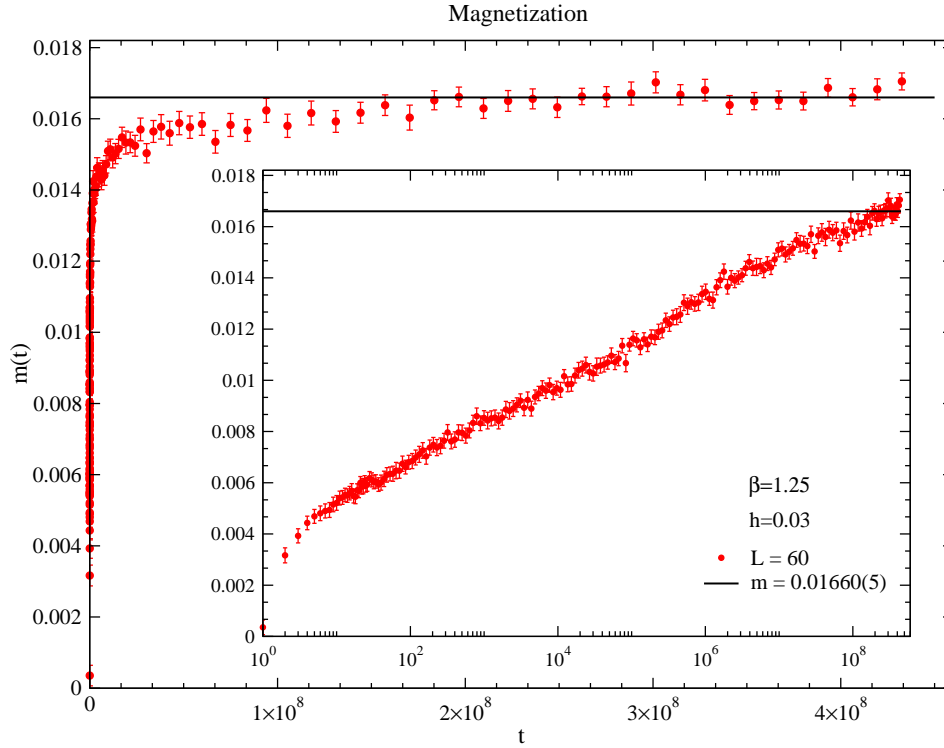


Figure 5. Magnetization as a function of time for $\beta = 1.25$, $L = 60$ and $h = 0.03$. We have plotted in the inset the main plot with logarithmic scale in the abscissas, in order to make sure we had found a plateau. We have marked in the main figure the plateau of the magnetization with a horizontal line.

We will show in this section plots corresponding to $\beta = 1.25$ and $L = 60$. In order to obtain numerically m_{asyn} we have performed a very large in-eld numerical simulation recording the value of the magnetization at the time t : $m(t)$. The asymptotic value is simply $m_{\text{asyn}} = m(1)$ (this observable shows really small dependence on L for the lattice sizes simulated in this paper). To avoid extrapolations we have continued the run until the magnetization shows a plateau (this means that the magnetization has reached its equilibrium value), and so we extract the value of m_{asyn} by computing the position of this plateau. For instance, we show in figure (5) the magnetization as a function of time for $\beta = 1.25$ and $L = 60$.

By computing the asymptotic value of the magnetization for different temperatures, we obtain a reliable estimate for the order parameter in the droplet theory. In Table 1 we report these values for the droplet theory estimates and, in addition, we write the values for the order parameter obtained in the first part of this paper, that we will denote in the rest of the paper as $q_{EA}^{\text{dyn}}(\beta)$.

We recall that the values of $q_{EA}^{\text{dyn}}(\beta)$ reported in Table 1 have small finite size effects (taking into account their error bars) as checked in figure (3). Moreover, we have found strong discrepancies between $q_{EA}^{\text{dyn}}(\beta)$ and q_{EA}^{droplet} for small temperatures.

We will describe in the rest of the paper our results for the violation of FDT out

	$q_{EA}^{dyn}(\tau)$	$q_{EA}^{droplet}$
1.25	0.6583 (34)	0.5573 (13)
1.00	0.5071 (31)	0.3957 (17)
0.95	0.3554 (7)	0.3404 (21)

Table 1. $q_{EA}(\tau)$ for $L = 60$ from $C(t; t_w)$ (obtained in the first part of the paper) and assuming droplet theory from $m(T=h)$. All the data showed in this table were obtained in a $L = 60$ lattice except for dynamical q_{EA} at $\tau = 0.95$ that was obtained simulating a $L = 30$ lattice.

of equilibrium.

In figure (6) we report the FD data out of equilibrium for one of the lowest temperature simulated. We have shown a vertical band which marks our estimate of q_{EA}^{dyn} , a straight line to monitor the departure of this linear behavior and a horizontal band which marks $m_{asym} T=h$ (see figure (5)). In addition we have plotted data from three different waiting times.

Figure (6) shows that our estimate for q_{EA}^{dyn} matches very well in the plot and marks the region in which the FD data starts to depart from the linear behavior (for all the temperatures simulated). In figure (7) we have drawn a magnification of this region. In addition, in this figure one can see that the finite time effects in the building of the asymptotic curve are small. Practically the two biggest waiting times are compatible in the error (there is a factor ten in waiting time). With the state-of-the-art dedicated computer of the day it is impossible to simulate larger waiting times. We can conclude from this figure that we are unable to see dependence in waiting time for the two largest waiting times in the region in which they depart from the linear behavior. The dependence on the waiting time for larger times is smaller than our statistical errors. From our numerical data a droplet theory Fluctuation-dissipation asymptotic curve seems unlikely.

6. CONCLUSIONS

We have studied numerically and out of equilibrium the three dimensional Ising spin glass with binodal disorder.

By computing the out of equilibrium spin-spin correlation function we have been able to extract the order parameter of the phase transition. The study of the behavior of this order parameter with temperature permit us to compute the critical temperature and the associated critical exponent: both figures compare very well with previous numerical simulations and experiments. We have also discarded a XY-like scenario (we have found a non-vanishing order parameter in the low temperature region). We have also monitored the dependence of $q_{EA}(\tau)$ with the lattice size in the low temperature region for one.

In the second part of the paper we have extracted the droplet prediction for the

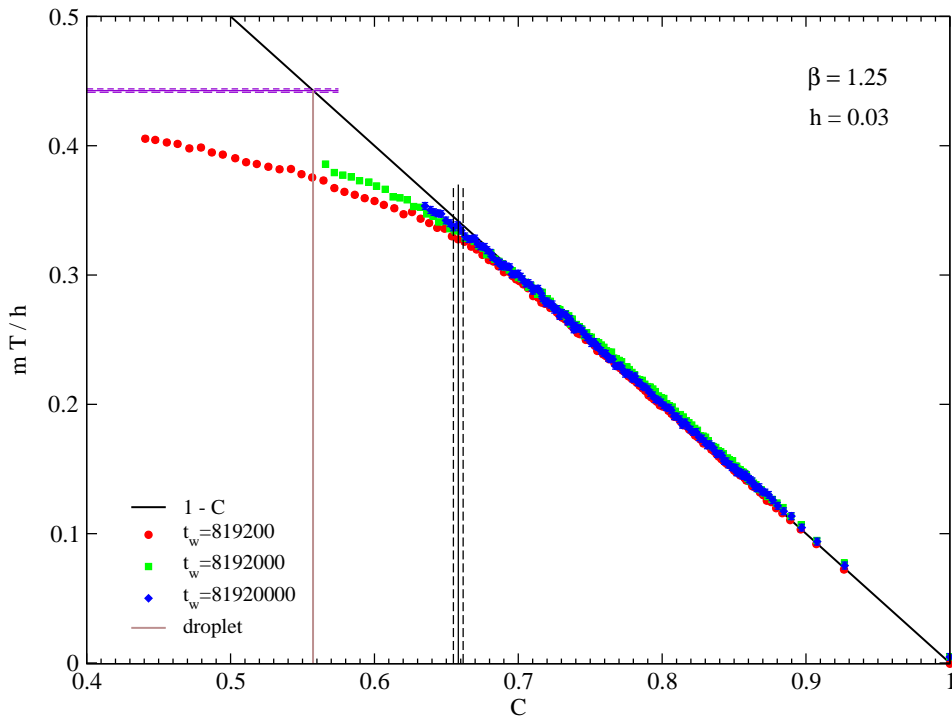


Figure 6. Fluctuation-dissipation curve out of equilibrium for one of the lowest temperatures simulated ($\beta = 1.25$, $L = 60$) and three waiting times. We have marked using three vertical lines the interval in which lies q_{EA}^{dyn} for this computed in the first part of the paper. In addition we have marked with three horizontal lines the value and the statistical error for $m_{asynt} T = h$. Finally we have marked a vertical line with the droplet theory prediction for q_{EA} (left part of the plot)

order parameter by computing the asymptotic value of the susceptibility ($mT = h$). The droplet prediction compares (for all the t_w 's simulated) well with the order parameter computed in the first part of the paper for high temperature (of course, slightly below the critical temperature), but for lower temperatures the comparison is bad.

Moreover the analysis (for larger waiting times) of the FD curves show a behavior that can be described in the RSB theory and points out that the droplet scenario seems unlikely (only a really small dependence on waiting time, outside of the precision of this work, could build a real FD curve compatible with the droplet theory). Moreover the point in which the numerical data depart from the linear behavior compares well with the estimate obtaining in the first part of this paper, supporting the RSB scenario.

Acknowledgments

This work has been partially supported by MEC (BFM 2003-C 08532, FISES2004-01399 and FIS2004-05073) and European Commission HPRN-CT-2002-00307. S. Perez Gavirio is a D.G.A. (Aragon Government) fellow.

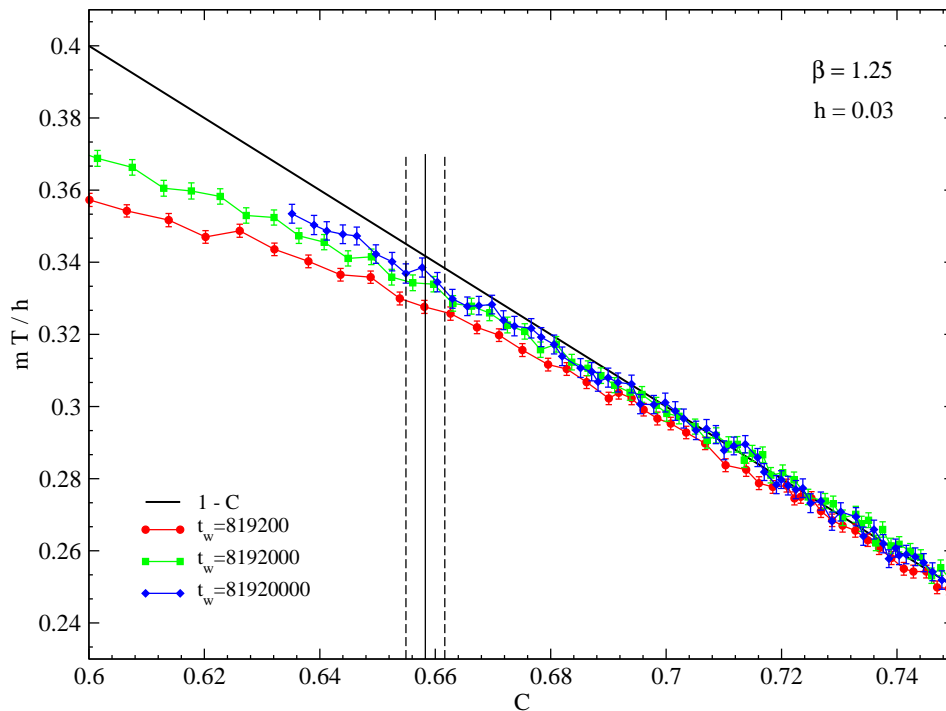


Figure 7. Magnification of figure 6 showing up the region in which the FD curves depart from the straight line $1 - C$. We have marked using three vertical lines the interval in which lies C_{EA}^{dyn} computed in the first part of the paper.

References

- [1] H. G. Ballesteros, A. Cruz, L. A. Fernandez, V. Martin-Mayor, J. Pech, J. J. Ruiz-Lorenzo, A. Taranco, P. Tellez, C. L. Ullod and C. Ungil, *Phys. Rev. B* **62**, 14237 (2000).
- [2] H. G. Katzgraber, M. Koerner, A. P. Young, cond-mat/0602212.
- [3] T. Jorg, cond-mat/0602215.
- [4] L. Berthier and J.-P. Bouchaud, *Phys. Rev. B* **66**, 054404 (2002).
- [5] E. Vincent, J. Hammann, M. Ocio, J.-P. Bouchaud and L. F. Cugliandolo, "Slow dynamics and aging in spin-glasses" in *Complex Behavior of Glassy Systems*. Springer Verlag 1997.
- [6] G. Parisi, F. Ricci-Tersenghi and J. J. Ruiz-Lorenzo, *Journal of Physics A: Math and Gen.* **29**, 7943 (1996).
- [7] D. A. Stariob, M. A. Montemurro, F. A. Tamari, *Eur. Phys. J. B* **32**, 361-367 (2003).
- [8] H. Yoshino, K. Hukushima, H. Takayama, *Phys. Rev. B* **66**, 064431 (2002).
- [9] L. F. Cugliandolo and J. Kurchan, *Phys. Rev. Lett.* **71**, 173 (1993); *Phil. Mag.* **71**, 501 (1995); *J. Phys. A* **27**, 5749 (1994).
- [10] S. Franz and M. Mezard, *Europhys. Lett.* **26**, 209 (1994).
- [11] A. Baldassarri, L. F. Cugliandolo, J. Kurchan and G. Parisi, *J. Phys. A* **28**, 1831 (1995).
- [12] E. Marinari, G. Parisi, F. Ricci-Tersenghi and J. J. Ruiz-Lorenzo, *J. Phys. A* **31**, 2611 (1998).
- [13] S. Franz and H. Rieger, *J. Stat. Phys.* **79**, 749 (1995).
- [14] S. Franz, M. Mezard, G. Parisi, L. Peliti, *Phys. Rev. Lett.* **81**, 1758 (1998); *J. Stat. Phys.* **97**, 459 (1999).
- [15] D. Herisson and M. Ocio, *Phys. Rev. Lett.* **88**, 257202 (2002).
- [16] M. Mezard, G. Parisi and M. A. Virasoro, *Spin glass theory and beyond*. World Scientific, Singapore 1987.

- [17] E. Marinari, G. Parisi, F. Ricci-Tersenghi, J. J. Ruiz-Lorenzo and F. Zuliani, *J. Stat. Phys.* 98, 973 (2000).
- [18] W. L. McMillan, *J. Phys. C* 17, 3179 (1984); A. J. Bray and M. A. Moore, in *Heidelberg Colloquium on Glassy Dynamics*, edited by J. L. Van Hemmen and I. Morgenstern (Springer Verlag, Heidelberg, 1986), p. 121; D. S. Fisher and D. A. Huse, *Phys. Rev. Lett.* 56, 1601 (1986); *Phys. Rev. B* 38, 386 (1988).
- [19] J. J. Ruiz-Lorenzo, "Low temperature properties of Ising spin glasses: (some) numerical simulations" in "Advances in Condensed Matter and Statistical Mechanics", Ed. E. Krutcheva and R. Cuerno. Published by Nova Science Publishers 2004. cond-mat/0306675.
- [20] D. Triguiez, E. Marinari, G. Parisi and J. J. Ruiz-Lorenzo, *J. Phys. A* 30, 7337 (1997).
- [21] G. Parisi, F. Ricci-Tersenghi and J. J. Ruiz-Lorenzo, *Eur. Phys. J. B* 11, 317-325 (1999).
- [22] A. Cruz, J. Pech, A. Tarancon, P. Tellez, C. L. Ullod and C. Ungil, *Comput. Phys. Commun.* 133, 165 (2001).
- [23] K. Gunnarsson, P. Svedlindh, P. Nordblad, L. Lundgren, H. Aruga and A. Ito, *Phys. Rev. B* 43, 8199 (1991).
- [24] M. Pleimling and I. A. Campbell, *Phys. Rev. B* 72, 184429 (2005). M. Henkel and M. Pleimling, *Europhys. Lett.* 69. 524 (2005).